

## Plate girders under bending

Abspoel, Roland

**Publication date**

2016

**Document Version**

Accepted author manuscript

**Published in**

proceedings of the International Colloquium on Stability and Ductility of Steel Structures

**Citation (APA)**

Abspoel, R. (2016). Plate girders under bending. In D. Dubina, & V. Ungureanu (Eds.), *proceedings of the International Colloquium on Stability and Ductility of Steel Structures: Timisoara, Romania* (pp. 1-8). Wiley.

**Important note**

To cite this publication, please use the final published version (if applicable).  
Please check the document version above.

**Copyright**

Other than for strictly personal use, it is not permitted to download, forward or distribute the text or part of it, without the consent of the author(s) and/or copyright holder(s), unless the work is under an open content license such as Creative Commons.

**Takedown policy**

Please contact us and provide details if you believe this document breaches copyrights.  
We will remove access to the work immediately and investigate your claim.



# PLATE GIRDERS UNDER BENDING

Roland Abspoel

*Delft University of Technology, Delft, The Netherlands*

**Abstract:** In a material economy driven plate girder design, the lever arm between the flanges will increase. This leads to higher stiffness and bending moment resistance, but also to an increase of the web slenderness. This means that high strength steels can be used leading to a large reduction of the steel consumption. However, Eurocode 3 [3] restricts the web slenderness based on the formula to avoid flange induced buckling, derived by Basler [2]. Experimental and theoretical research by Abspoel [1] conducted at the Stevin II Laboratory of Delft University of Technology, shows that this formula is too conservative. Ten unstiffened plate girders with high web slenderness's are tested, focussed on flange induced buckling.

## 1. Introduction

In many steel structures like buildings, industrial halls and bridges, standard hot-rolled sections are used. These sections are divided into specific types, such as IPE, HEA, HEB, HEM, HED and UNP in Europe and similar profiles in the USA. The range of hot-rolled sections is limited and therefore fabricated plate girders are used when the standard hot-rolled sections do not meet the requirements for stiffness, strength, stability and economy.

Such a plate girder is built up from steel plates for the top and bottom flange and for the web, welded together to an I-shape cross-section, single or double symmetric. Using this type of plate girders, a high degree of optimisation of material use is achieved by using different plate thicknesses and widths for the flanges, and thickness and height for the web over the span of the girder adapted to the distribution of bending moments and the shear forces.

Optimisations can be carried out for many aspects, but in the PhD-thesis by Abspoel [1] the ultimate bending moment resistance of a plate girder, given a certain weight per unit length, is the main topic for optimisation. For a long time, this was not or hardly of interest at all in Western countries, especially because the cost of structures was mainly determined by labour cost and hardly by material cost. Due to the increasing automation in the production of plate girders, the material cost becomes more important than the labour cost. However, for

nowadays structures, life cycle costs and the environmental impact of structures become of greater influence on the design, beside to the increasing cost of steel by expanding demand by booming economies like China, Brazil, India and other upcoming economies. So, optimisation for minimal use of materials has become highly important.

Using higher steel grades, applying most material in the flanges and increasing the lever arm between both flanges are the main possibilities to maximise the bending moment resistance of a plate girder under pure bending given a certain amount of steel.

In case of a fixed cross-sectional area, by increasing the lever arm, more material is placed in the web, reducing the remaining material for the flanges. However, the lever arm can also be increased without using more material in the web by increasing the web height and decreasing the web thickness. This process is restricted by a limit for a practical thickness of the web, to enable welding of the section and also the handling of the plate girder.

The slenderness of the flanges, expressed in the width to thickness ratio of the flange plate, is restricted such that at least yielding of the outer fibre is possible to ensure that the plate girder exhibits at least a “not brittle-like” post-critical behaviour.

However, EN 1993-1-5 [3] limits the web slenderness by a specific phenomenon called “flange induced buckling”. This phenomenon has been studied by Basler [2] and described as “vertical buckling of the compressive flange into the web”.

Basler based this maximum web slenderness only on one laboratory test result and so it was considered of interest to perform additional research on this limitation to investigate whether this phenomenon really limits the bending moment resistance of a plate girder and to see if it is possible to increase this maximum web slenderness.

## 2. Vertical buckling of the compressive flange into the web

Basler [2] developed a model to determine the maximum web slenderness, based on vertical buckling of the compressive flange into the web. The curvature of the test panel of the plate girder under pure bending is constant. It is assumed that the compressive flange yields and because of this curvature a stress perpendicular to the flange  $\sigma_n$  acts on the web, see Fig. 1.

$$\sigma_n = A_{tf} \cdot f_{y,tf} \cdot \frac{2 \cdot \varepsilon_{tf}}{h \cdot t_w} \approx \frac{A_{tf}}{A_w} \cdot 2 f_{y,tf} \cdot \varepsilon_{tf} = \sigma_{cr} = \frac{\pi^2 E}{12 \cdot (1 - \nu^2) \cdot \left( \frac{h_w}{t_w} \right)^2} \quad (1)$$

The strain of the top flange is assumed to be larger than the yield strain,  $\varepsilon_{tf} \geq \varepsilon_{y,tf}$ , because it is required that the flange fully yields to obtain some deformation capacity to guarantee that the compressive flange will fully yield. To be sure  $\varepsilon_{tf} \geq \varepsilon_{y,tf}$ , the strain  $\varepsilon_{tf}$  of the top flange is taken equal to  $\varepsilon_{tf} = (f_{y,tf} + \sigma_r) / E$ , where  $\sigma_r$  is the residual stress in the compressive flange.

$$\beta_{w,max,I} = \frac{h_w}{t_w} = \sqrt{\frac{\pi^2 E}{24 \cdot (1 - \nu^2)} \cdot \frac{A_w}{A_{tf}} \cdot \frac{1}{f_{y,tf} \cdot \frac{f_{y,tf} + \sigma_r}{E}}} = 0.67 \cdot \sqrt{\frac{A_w}{A_{tf}}} \sqrt{\frac{E^2}{f_{y,tf} \cdot (f_{y,tf} + \sigma_r)}} \quad (2)$$

This is the most general equation for the maximum web slenderness  $\beta_{w,max}$ . By assuming minimum values for the ratio of area  $A_w / A_f$ , but also by assuming a minimum for the residual stress  $\sigma_r$  in the compressive flange, this equation can be simplified.

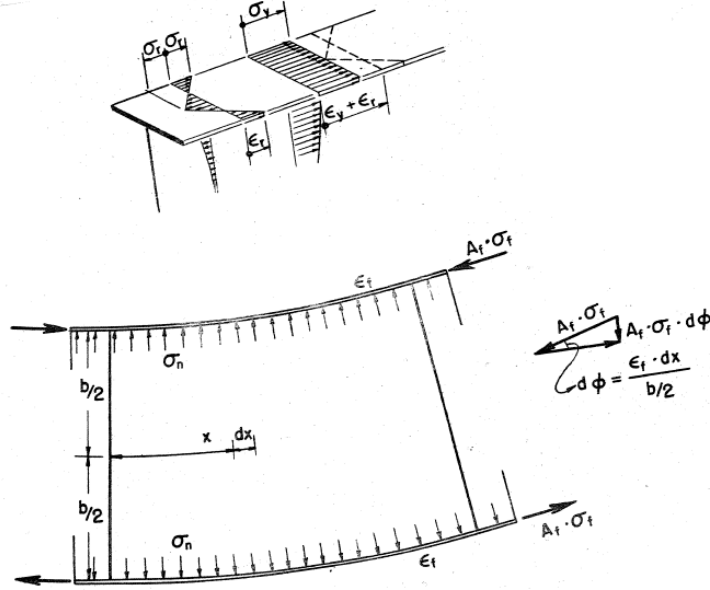


**Fig. 1:** Determination of the maximum web slenderness according to Basler [2]

Basler [2] mentioned that the ratio of area  $\rho = \frac{A_w}{A_f}$  shall not be taken smaller than 0.5. Substitution of the ratio of area  $\rho = 0.5$  in Eqn. (2), gives for the maximum web slenderness  $\beta_{\max}$ :

$$\beta_{w.\max.II} = \frac{0.48E}{\sqrt{f_{y.tf} \cdot (f_{y.tf} + \sigma_r)}} \quad (3)$$

A second simplification of Eqn. (2) is found by assuming a residual stress level of  $\sigma_r = \frac{f_{y.tf}}{2}$  for mild steel and so the maximum web slenderness  $\beta_{w.\max}$  becomes:

$$\beta_{w.\max.III} = \sqrt{\frac{\pi^2}{36 \cdot (1 - \nu^2)}} \cdot \frac{E}{f_{y.tf}} \cdot \sqrt{\frac{A_w}{A_f}} = 0.55 \cdot \frac{E}{f_{y.tf}} \cdot \sqrt{\frac{A_w}{A_f}} \quad (4)$$

In EN1993-1-5 [3] this Eqn. (4) is used. Vertical buckling of the compressive flange into the web is called “flange induced buckling”. A third simplification of the maximum web slenderness  $\beta_{w.\max}$  is given by taking into account a ratio of area  $\rho = 0.5$  as well as a residual stress level of  $\sigma_r = \frac{f_{y.tf}}{2}$ . The maximum web slenderness  $\beta_{w.\max}$  as given in Eqn. (2), changes into:

$$\beta_{w.\max.IV} = \frac{0.40E}{f_{y.tf}} \quad (5)$$

In EUR 8849 [4], a draft Eurocode, the equation for the maximum web slenderness  $\beta_{w.\max}$  is presented as given in Eqn. (6). For mild steel S235, the maximum web slenderness is 360.

Test specimen G4-T2 failed by vertical buckling of the compressive flange. The actual web slenderness of girder G4 was  $\beta_w = h_w/t_w = 1270/3.3 = 387.6$  and the actual ratio of area was

$$\rho = \frac{A_w}{A_f} = \frac{h_w \cdot t_w}{b_{tf} \cdot t_{tf}} = \frac{1270 \cdot 3.3}{308.9 \cdot 19.7} = 0.69. \text{ The actual maximum web slenderness } \beta_{w.\max} \text{ based on}$$

this ratio of area  $\rho = A_w/A_f = 0.69$  according to Eqn. (4) is determined with:

$$\beta_{w,max} = 0.55 \cdot \frac{E}{f_{y,tf}} \cdot \sqrt{\frac{A_w}{A_f}} = 0.55 \cdot \frac{206000}{259.2} \cdot \sqrt{0.69} = 368.3$$

The web slenderness  $\beta_w$  of test specimen G4-T2 is larger than the maximum web slenderness  $\beta_{w,max}$  and so there will be vertical buckling of the flange into the web. The strain was “slightly” higher than the yield strain  $\varepsilon_y$ . The actual strengths and areas of test specimen G4-T2 are given in Table 1, including the actual web slenderness  $\beta_w$  and the actual maximum web slenderness  $\beta_{w,max.III}$  based on Eqn. (3) and  $\beta_{w,max.IV}$  based on Eqn. (4).

Table 1

	$A_{tf}$ [mm <sup>2</sup> ]	$f_{y,tf}$ [MPa]	$A_w$ [mm <sup>2</sup> ]	$\beta_{w,max.III}$ [-]	$\beta_{w,max.IV}$ [-]	$\beta_w$ [-]
G4-T2	6072.1	259.2	4161.2	368.3	324.3	387.6

### 3. Delft experiments

In Fig. 2 a schematic presentation of the test setup is given.

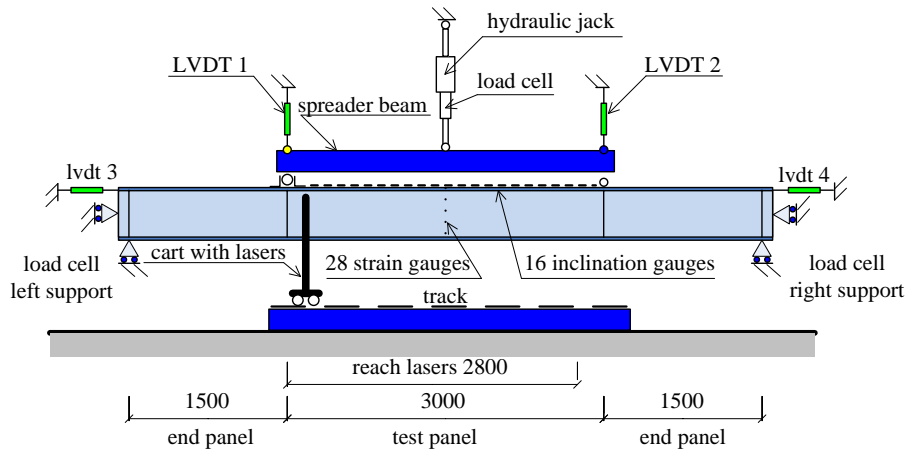


Fig. 2: Schematic presentation of a test specimen and the test rig

The web slenderness  $\beta_w$  of interest lies between 400 and 800, related to commonly used ratios of areas  $\rho$ , between  $\frac{1}{2}$  and 2 according to Basler [2]. Based on the maximum web slenderness  $\beta_{w,max}$ , see Eqn. (4), the web slenderness  $\beta_w$  lies between 360 and 720. Because of the shift of the neutral axis due to the use of the effective width method, these web slenderness's are taken higher than described by Basler, namely between 400 and 800.

To make such relatively large objects more suitable for testing in a laboratory, the dimensions are scaled down to a web thickness of 1 mm and a span of 6000 mm for all 10 test specimens. Based on this web thickness  $t_w = 1 \text{ mm}$ , web heights of 400 mm, 600 mm and 800 mm are used, which leads to a web slenderness  $\beta_w$  of 400, 600 and 800 respectively.

Related to the limitation of the ratios of area between  $\frac{1}{2}$  and 2 the cross-sectional area of the flanges is taken 200 mm<sup>2</sup> and 400 mm<sup>2</sup> and the following flange dimensions are taken: 50×4 mm<sup>2</sup>, 80×5 mm<sup>2</sup> and 100×4 mm<sup>2</sup>. The last two flanges have the same flange area  $A_f$ , but different flange dimensions. Especially, because of the difference in flange thicknesses

$t_f$ , the torsional stiffness's  $EI_t$  differ, based on  $b \cdot t_f^3$ . The actual geometrical dimensions of the test specimens are given in Table 2. The maximum web slenderness is according to Eqn. (4) and based on the actual yield stresses, for test girder 9, 800×80,  $f_{y,tf} = 320 \text{ MPa}$ .

Table 2

	$h_w$ [mm]	$t_w$ [mm]	$b$ [mm]	$t_f$ [mm]	$\beta_w$ [-]	$\beta_{w,max}$ [-]	$\rho$ [-]
1, 400×50	400	1.0	50	4	400	471.2	2.0
2, 400×80(1)	400	1.0	80	5	400	344.7	1.0
3, 400×80(2)	400	1.0	80	5	400	349.6	1.0
4, 400×100	400	1.0	100	4	400	315.7	1.0
5, 600×50	600	1.0	50	4	600	585.0	3.0
6, 600×80	600	1.0	80	5	600	403.1	1.5
7, 600×100	600	1.0	100	4	600	395.5	2.5
8, 800×50	800	1.0	50	4	800	664.2	4.0
9, 800×80	800	1.0	80	5	800	476.8	2.0
10, 800×100	800	1.0	100	4	800	470.7	2.0

#### 4. Measurements on the test panel of test girder 9, 800×80

The results of test girder 9, 800×80, are shown in this section. For the results of the remaining nine test girders see Abspoel [1]. Fig. 3 shows the  $P$ - $\delta$  diagram of the test girder, based on the actuator force and the deformations of the piston. It can be seen that the girder finally fails after reaching the maximum force in deformation step H.

The total out-of-plane deflections of the web in the test panel are measured by using lasers on a movable cart, see Figs. 4, 5 and 6 for respectively deformation step 0, H and I. Next to these total out-of-plane deflections of the web, the out-of-plane deformations as function of the load can be seen in Figs. 7 and 8 and finally, Figs. 9, 10 and 11 show the increment of the out-of-plane deflections.

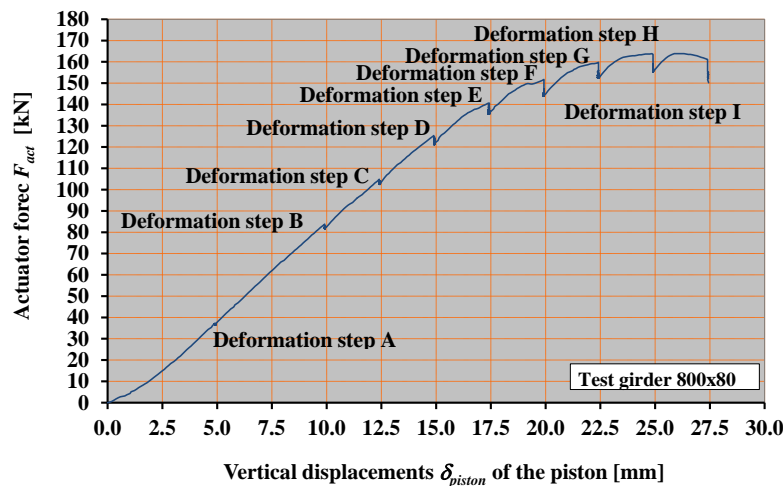
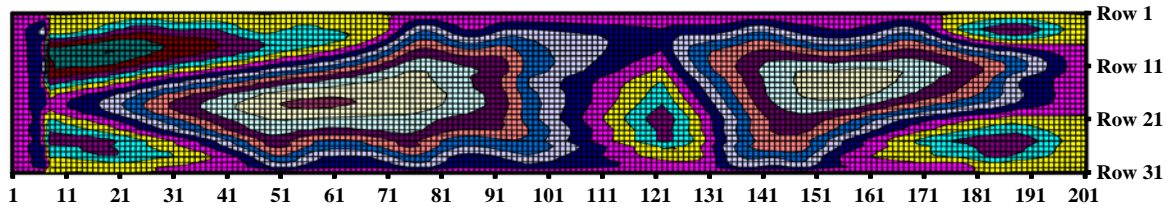
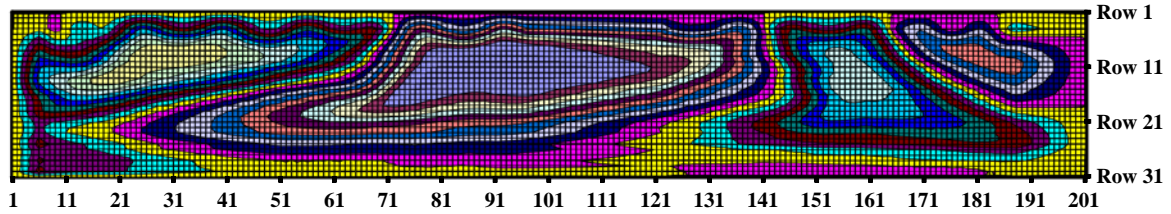


Fig. 3: The actuator force as result of the prescribed displacements of the piston



**Fig. 4:** Initial total out-of-plane displacements, deformation step 0



**Fig. 5:** Total out-of-plane displacements, deformation step H

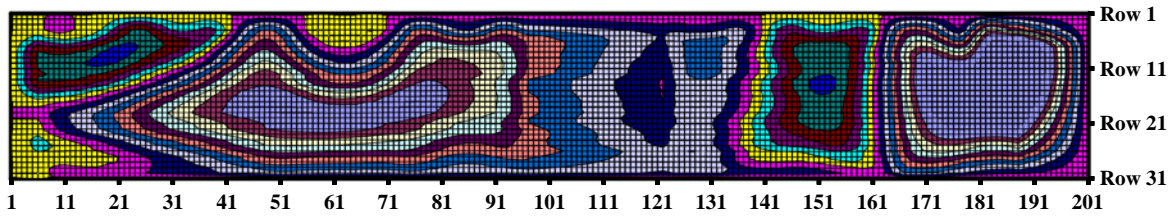


**Fig. 6:** Total out-of-plane displacements, deformation step I

From Figs. 4 to 6 it can be seen that the total out-of-plane deflections of the web in the test panel is asymmetric over the span of the test panel. The maximum load is reached for deformation step H and in the next deformation step the pattern of the deflections changed suddenly and the girder fails. Figs. 7 and 8 show that at the right side of the test panel one big buckle is subdivided into two buckles, a snap through. Figs. 9 and 10 show that in deformation step I almost the whole web buckles.

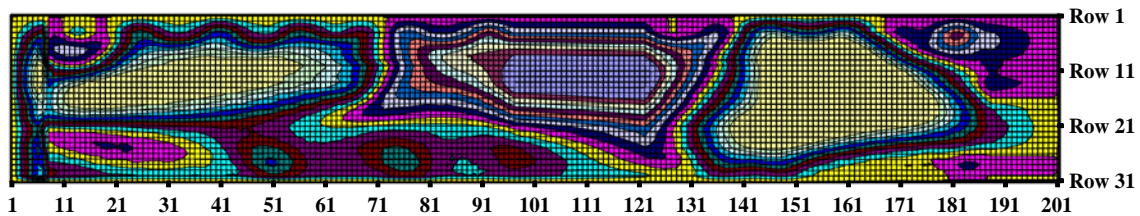


**Fig. 7:** The out-of-plane deflections as function of the loading in deformation step H

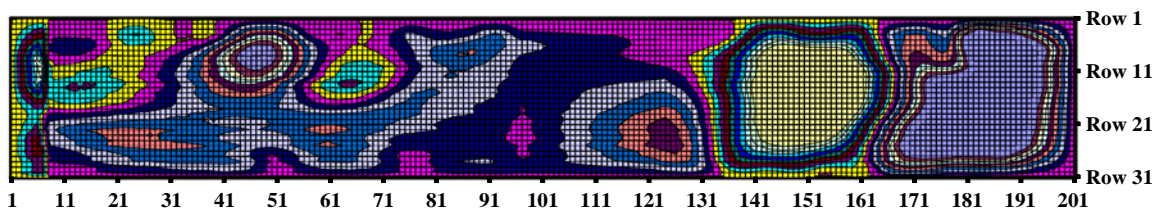


**Fig. 8:** The out-of-plane deflections as function of the loading in deformation step I

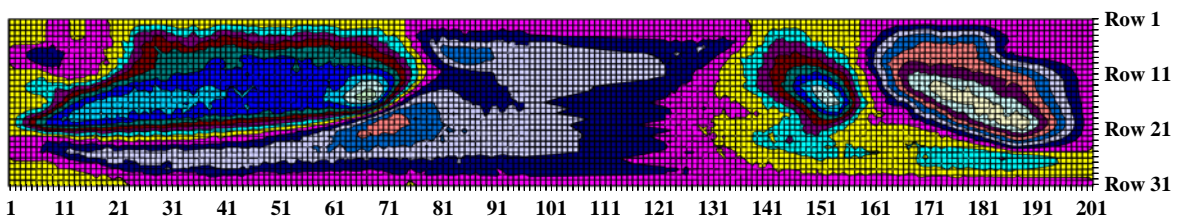


**Fig. 9:** The increment in the out-of-plane deflections, deformation step H

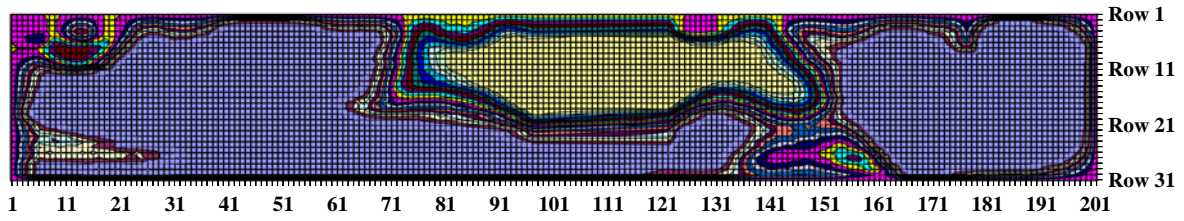


**Fig. 10:** The increment in the out-of-plane deflections, deformation step I

Table 3 shows the vertical deflections at the load introductions, measured by two Lvdts at the top of the spreader beam, for all test girders for step the maximum load appears.

Table 3

	$\delta_{z,Lvdt1}$ [mm]	$\delta_{z,Lvdt2}$ [mm]	$\Delta\delta_z$ [mm]
1, 400×50	27.14	26.59	-0.55
2, 400×80(1)	31.86	32.59	+0.73
3, 400×80(2)	40.27	41.61	+1.34
4, 400×100	37.28	36.41	-0.87
5, 600×50	31.30	25.44	-5.86
6, 600×80	22.25	22.29	+0.04
7, 600×100	23.55	23.90	+0.35
8, 800×50	20.87	22.29	+1.40
9, 800×80	18.63	19.76	+2.13
10, 800×100	18.63	20.87	+2.61

From Table 3 it can be seen that there is hardly any difference in vertical deflection at both load introductions and so it can be concluded that flange induced buckling is not determining the maximum load. Even a maximum difference of 5.86 mm is rather small over the length of 3.0 m of the test panel. Fig. 11 shows the vertical deflection over the span of the test panel for every deformation step for test girder 9, 800×80. It can be seen, that the girder deforms asymmetric in deformation step I, so after the load is a maximum in the  $P$ - $\delta$  diagram in deformation step H.

The bending moment resistance of this test girder 9, 800×80, is rather close to the bending moment resistance based on the cross-section existing of only the flanges, but also close to the effective bending moment resistance taking into account partly yielding of the web. The yield stress of all webs is smaller than the yield stress of the flanges.

## 5. Conclusions

The following conclusions can be drawn:

1. The model for vertical buckling of the compressive flange into the web as adopted in the EN 1993-1-5 [3] and in the AISC 360-10 [5] is much too conservative according to the test results. This can be caused by the assumption related to the residual stresses, the assumption that the web is simply supported by the flanges, the way the curvature is calculated, the neglect of the influence of the stresses due to bending;
2. It can be concluded that the maximum web slenderness is larger than 800 up to S355, based on actual yield stresses, which is, related to the application of plate girders, very high;

3. For cases where the deflections criterion is not governing, it is concluded that possible material savings obtained by using high strength steel grades and by optimising the cross-section of plate girders are possible up to approximately 50%. This is an important finding for reducing the carbon footprint of steel structures.

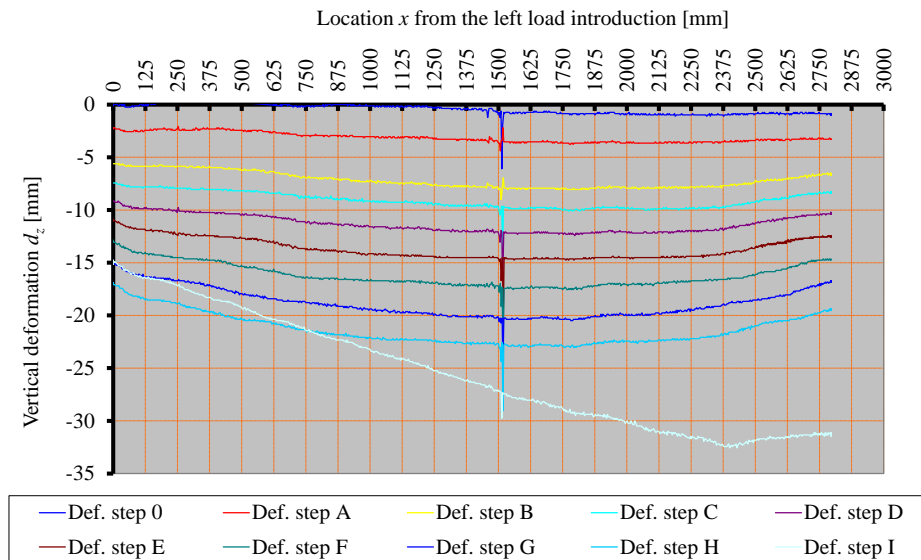


**Fig. 11:** Vertical deformations between both load introductions

## References

- [1] Abspoel R. “Optimisation of plate girders”, *Dissertation*, Delft, The Netherlands, 2015.
- [2] Basler K. “Strength of plate girders”, *Dissertation*, Bethlehem, America, 1959.
- [3] EN 1993-1-5, *Eurocode 3: Design of steel structures – Part 1-5 Plated structural elements*, 2006.
- [4] EUR 8849, *Draft Eurocode 3: Common unified rules for steel structures*, 1984
- [5] AISC 360-10, *Specification for structural steel buildings*, American Institute of Steel Constructions, 2010.